iopolymer Applications Journal
e-ISSN: 2800-1729

Hayet Ahlem Lezrag et al. Vol 5 N° 2, 2026, pp. 21-29

Niosomal Encapsulation of *Artemisia herba-alba* Essential Oil: Optimization and Characterization Using Box-Behnken Design

Hayet Ahlem Lezrag[1. 2. 3*] ; Sofiane Fatmi[1. 2. 4*] ; Zahra Toutou[1. 2] ; Katarzyna Pokajewicz[3] ; Mohamed Skiba[4] ; Piotr P. Wieczorek[3] and Mokrane Iguerouada[1]

1: Université de Bejaia. Faculty of Nature and Life Sciences. Associated Laboratory in Marine Ecosystems and Aquaculture. 06000 Bejaia. Algeria
2: Université de Bejaia. Faculty of Technology. Technology Pharmaceutical Laboratory. 06000 Bejaia. Algeria.
3: University of Opole. Institute of Chemistry. 45-052 Opole. Poland.
4: Technology Pharmaceutical and Bio Pharmaceutics Laboratory. UFR Medicine and Pharmacy. Rouen University. 22 Blvd. Gambetta. 76183. Rouen. France.
**Corresponding author email: sofiane.fatmi@univ-bejaia.dz, hayetahlem.lezrag@univ-bejaia.dz*

Received: 9 June 2026; Accepted: 1 July 2026.; Published: 13 July 2026

Abstract

This study focuses on the development and optimization of niosomal vesicles for the encapsulation of Artemisia herba-alba (white wormwood) essential oil, a plant native to arid and semi-arid regions of Algeria. A Box-Behnken experimental design was employed to investigate the effects of cholesterol concentration, Span 60 concentration, and sonication time on niosome size and encapsulation efficiency. The optimal formulation was achieved using 0.25 µL/mL of essential oil, 2.5 mg/mL of cholesterol, 5.8 mg/mL of Span 60, and a sonication time of 7 min, resulting in an experimental encapsulation efficiency of 90.67% with an average particle size of 880 nm. Fourier-transform infrared spectroscopy (FTIR) confirmed the physical nature of encapsulation through hydrogen bonding interactions without chemical modification of components. X-ray diffraction (XRD) analysis revealed a decrease in crystallinity of excipients, indicating successful integration of the essential oil into the niosomal bilayer. Stability studies demonstrated progressive physical instability with particle growth from 880 nm to 2780 nm over 90 days, while encapsulation efficiency remained above 83%. These findings establish niosomes as an effective vectorization system for A. herba-alba essential oil, enhancing its stability and offering promising applications in pharmaceutical and nutraceutical fields.

Keywords: *Artemisia herba-alba, essential oil, niosomes, Box-Behnken design, FTIR, XRD.*

I. Introduction

Essential oils represent a valuable source of bioactive compounds with demonstrated antimicrobial, antioxidant, anti-inflammatory, and therapeutic properties [1]. Among aromatic and medicinal plants. Artemisia herba-alba Asso (white wormwood, Asteraceae) occupies a prominent position in traditional medicine across North Africa and the Mediterranean basin. This perennial shrub, characteristic of arid and semi-arid steppic ecosystems. produces an essential oil rich in oxygenated monoterpenes, particularly camphor (39.5%), chrysanthenone (10.4%), and 1.8-cineole (8.6%) alongside α-thujone (7.0%) and borneol (3.4%) [2]. These terpenic compounds confer potent antioxidant. antibacterial. antifungal, and anti-inflammatory activities [3].

Despite their therapeutic potential, essential oils present significant limitations that restrict their pharmaceutical applications high volatility, poor water solubility, chemical instability under environmental stressors (light, oxygen, temperature), and potential toxicity at elevated concentrations [4]. These constraints necessitate the development of advanced drug delivery systems capable of protecting. stabilizing, and controlling the release of these bioactive molecules.

Niosomes (non-ionic surfactant vesicles) have emerged as promising nanocarriers for the encapsulation of both hydrophilic and lipophilic compounds [5]. Composed of non-ionic surfactants (typically Span series) and cholesterol, niosomes offer several advantages over conventional liposomes enhanced chemical stability, lower production costs, absence of special storage requirements, and reduced toxicity [6]. Their bilayer structure enables the encapsulation of lipophilic compounds such as essential oils within the hydrophobic membrane domain, thereby improving solubility. bioavailability and controlled release [7].

The optimization of niosomal formulations requires systematic evaluation of multiple formulation variables. Response surface methodology (RSM), particularly the Box-Behnken design (BBD). Provides an efficient statistical approach for studying the effects of independent variables and their interactions on multiple responses with a reduced number of experimental runs [8]. This design has been successfully applied to optimize niosomal formulations for various drugs and natural compounds [9.10].

The present study aims to develop and optimize niosomal formulations for A. herba-alba essential oil using BBD,characterize the optimized formulation through FTIR spectroscopy and XRD analysis and evaluate the stability of niosomal vesicles during storage.

This work represents, to our knowledge, the first systematic optimization of niosomal encapsulation for Algerian A. herba-alba essential oil using a quality-by-design approach.

II. Material and methods

II.1. Materials

Artemisia herba-alba essential oil was obtained by hydrodistillation of aerial parts collected in the region of Bordj Bou Arreridj, Northeastern Algeria. during the flowering stage, Span 60 (sorbitan monostearate) and cholesterol were purchased from Sigma-Aldrich (St. Louis. MO. USA). Absolute ethanol. were obtained from Biochem Chemopharma (Canada). All reagents were of analytical grade.

II2. Isolation of essential oil from Artemisia herba-alba

Artemisia herba-alba. commonly known as white wormwood. is a plant species native to arid and semi-arid regions. The fresh aerial parts of A. herba-alba were collected in Northeastern Algeria. specifically in the region of Bordj Bou Arreridj. during the flowering stage. After harvesting. The plant material was roughly chopped, air-dried, and then subjected to hydrodistillation for 4 hours using a Clevenger-type apparatus. The resulting essential oil was collected and stored at 4 °C in the dark until further analysis and experimental use [11].

II.3. Preparation of niosomal formulations

Niosomes were prepared using the ethanol injection method [12]. Briefly, Span 60, cholesterol. and A. herba-alba essential oil were dissolved in absolute ethanol to form the organic phase. This solution was maintained under magnetic stirring at 60 °C for 20 min to ensure complete dissolution. The organic phase was then injected into the aqueous phase (preheated to 60 °C) using a syringe. with continuous stirring. Residual ethanol was removed by rotary evaporation under reduced pressure. The resulting suspension was sonicated using a bath sonicator (Sonitech. ST-80 PRO) for the designated time period to obtain homogeneous niosomes.

II.4. Box-Behnken experimental design

Optimization of the niosomal formulation was carried out using a three-factor, three-level Box–Behnken design (BBD) implemented in MODDE 6.0 software (Umetrics AB, Sweden) [13]. Cholesterol concentration (X_1, 1–5 mg/mL), Span 60 concentration (X_2, 5–15 mg/mL), and sonication time (X_3, 2–7 min) were selected as independent variables based on their expected influence on vesicle formation and stability. Encapsulation efficiency (Y_1, %) and particle size (Y_2, nm) were chosen as response variables to evaluate formulation performance. The design generated a total of 15 experimental combinations, including three center-point replicates, allowing estimation of pure error, evaluation of model adequacy, and assessment of experimental reproducibility. The actual and coded values of the investigated factors are presented in Table 1.

Table 1. Variables and levels in Box-Behnken design

Factor	Symbol	Units	Low (-1)	Center (0)	High (+1)
Cholestérol	Cho (X_1)	mg/mL	1	3	5
Span 60	Spa (X_2)	mg/mL	5	10	15
Sonication time	Son (X_2)	min	2	4.5	7

II.5. Niosome size determination

The particle size of the niosomal suspensions was determined by optical microscopy using an ocular micrometer calibrated with an objective micrometer. Briefly, a drop of the niosomal suspension was placed on a clean microscope slide and covered with a coverslip. The calibrated ocular micrometer enabled direct measurement of vesicle diameters, with the micrometric divisions converted into length units using the established calibration factor. For each formulation, the diameters of at least 100 individual vesicles were measured to ensure statistical reliability, and the mean particle size was subsequently calculated [13].

II.6. Characterization of optimized formulation

II.6.1 Determination of encapsulation efficiency

Encapsulation efficiency (EE) was determined using a centrifugation-based separation method. The niosomal suspensions were centrifuged at 15,000 rpm for 90 min at 4 °C to ensure efficient separation of vesicles from the non-encapsulated essential oil. The low temperature was maintained to minimize the volatilization and potential degradation of the essential oil components during centrifugation. Following centrifugation, the supernatant

containing the free (non-encapsulated) essential oil was carefully collected and removed The resulting pellet [13]. Corresponding to the niosomal fraction, was dissolved in ethanol to disrupt the vesicular structure and release the encapsulated essential oil. The amount of encapsulated oil was then quantified by UV-visible spectrophotometry at 287 nm using a previously established calibration curve. Encapsulation efficiency was calculated according to the following equation:

$$EE\ (\%) = \frac{\text{Amount of encapsulated essential oil}}{\text{Total initial amount of essential oil}} \times 100$$

2.6.2. Fourier transform infrared spectroscopy (FTIR)

Fourier-transform infrared (FTIR) spectra were recorded using a Shimadzu UV-1900i spectrophotometer over the spectral range of 4000–400 cm^{-1}. The analyzed samples included Artemisia herba-alba essential oil, Span 60, cholesterol, the physical mixture, placebo niosomes, blank niosomes, and essential oil-loaded niosomes. Samples were prepared either as KBr pellets or as liquid films in the case of the essential oil. The obtained spectra were comparatively analyzed to identify potential intermolecular interactions among formulation components and to verify the successful encapsulation of the essential oil within the niosomal vesicles.

2.6.3. X-Ray diffraction (XRD)

XRD analysis was performed using a PANalytical Empyrean diffractometer equipped with Cu Kα radiation (λ = 1.5418 Å). Diffractograms were recorded over a 2θ range of 2° to 80°, with a step size of 0.02° and a scan speed of 5°/min. The resulting patterns of the pure components (Span 60, cholesterol, essential oil), the physical mixture, the placebo formulation, and the essential oil-loaded niosomes were subsequently compared.

2.7. Stability studies

The optimized niosomal formulation and the placebo were stored at temperature of (4°C ± 2 °C) for a period of 90 days. The physical stability of the formulations was evaluated by monitoring particle size and encapsulation efficiency at predetermined time intervals (0, 15, 30, 60, and 90 days).

III. Results and discussion

III.1. Calibration curve

A calibration curve for Artemisia herba-alba essential oil was established in ethanol at 287 nm. The calibration line passed through the origin and followed a linear equation of the form $y = a_* x$, where y represents the absorbance and x the essential oil concentration (µL/mL). The resulting regression equation was y = 1.0264x, with a coefficient of determination (R^2 = 0.9991). The absorbance–concentration relationship (Abs = f(C)) demonstrated excellent proportionality over the investigated concentration range (0–0.9 µL/mL). The high R^2 value, approaching unity, confirmed the strong linear correlation between absorbance and essential oil concentration, thereby validating compliance with the Beer–Lambert law and supporting the suitability of the method for quantitative analysis.

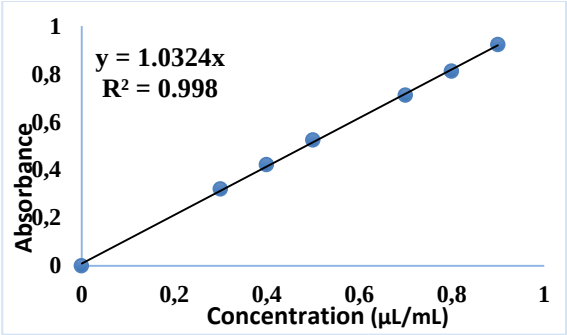

Figure 1. Artemsiia herba alba calibration curve.

III.2. Experimental design results

The experimental matrix and responses for the 15 runs are presented in Table 2. Encapsulation efficiency ranged from 48.00% to 98.66%. while niosome size varied from 630 nm to 1020 nm.

Run	X_1 (Chol)	X_2 (Span)	X_3 (Son)	EE (%)	Size (nm)
1	1	5	4.5	77.33	770
2	5	5	4.5	96.00	1020
3	1	15	4.5	56.00	725
4	5	15	4.5	64.00	870
5	1	10	2	58.66	890
6	5	10	2	64.00	990
7	1	10	7	72.00	630
8	5	10	7	93.33	930
9	3	5	2	72.00	1010
10	3	15	2	48.00	880
11	3	5	7	98.66	808
12	3	15	7	66.70	760
13	3	10	4.5	85.33	820
14	3	10	4.5	92.00	852
15	3	10	4.5	80.00	810

Table 2. Box-Behnken design matrix and experimental responses.

The highest encapsulation efficiency (98.66%) was achieved at run 11 with low cholesterol (1 mg/mL), low Span 60 (5 mg/mL) and high sonication time (7 min). However, the optimal compromise between size and encapsulation efficiency was identified through mathematical modeling.

The results indicate that the incorporation of Span 60 promotes the formation of larger and more stable niosomal vesicles, which can be attributed to its long saturated alkyl chain. This surfactant enhances the encapsulation efficiency of hydrophobic bioactive compounds, such as propolis, owing to its pronounced hydrophobic character and its ability

to increase bilayer rigidity, thereby improving membrane stability and drug retention [13]. Similar results was found by Fatmi et al [14]. When investigating the release characteristics of vitamin E and its protective role in maintaining sperm motility,encapsulated in liposome, cyclodextrin or polyethylene glycol.

III.3. Mathematical modeling and statistical analysis

The modeling using the Box-Behnken experimental design allowed us to obtain the following models:

$Y=a_0+a_1x_1+a_2x_2+a_3x_3+a_{11}x_{1^2}+a_{22}x_{2^2}+a_{33}x_{3^2}+a_{12}x_1x_2+a_{13}x_1x_3+a_{23}x_2x_3$

$\mathbf{Y= a_0 + a_1cho_l + a_2\ span + a_3\ son + a_{11}\ chol^2 + a_{22}\ span^2 + a_{33}son^2 + a_{12}\ chol*span + a_{13}chol*son + a_{23}span*son.}$

Y: estimated response.

$\mathbf{a_0}$: constant.

$\mathbf{a_1x_1.\ a_2x_2.\ a_3x_3}$: linear effects.

$\mathbf{a11x1^2.\ a_{22}x_2^2.\ a_{33}x_3^2}$**:** quadratic effects.

$\mathbf{a_{12}x_1x_2.\ a_{13}x_1x_3.\ a_{23}x_2x_3}$**:** interactions between factors.

For niosome size:

Size=827.333+99.375Cho46.625Sp80.25Son+7.20832Cho²+11.7084Spa²+25.4585Son²26.2501Cho*Spa+50Cho*Son+20.5001Spa*Son.

For encapsulation efficiency:

EE (%) = 85.7767+6.6675Cho-13.6613Spa+11.0038Son-5.89332Cho²6.55083Spa²7.88582Son²2.66751Cho*Spa+3.9975Cho*Son-1.99Spa*Son.

As shown in Table 3, the statistical analysis validated the adequacy and predictive reliability of both response surface models. The high determination coefficients obtained for vesicle size (R^2 = 0.994) and encapsulation efficiency (R^2 = 0.979) reflected excellent agreement between observed and predicted values. Likewise, the elevated Q^2 values (0.983 and 0.945, respectively) confirmed the strong predictive power of the models. Furthermore, the non-significant lack-of-fit ($p > 0.05$) indicated that the models accurately described the experimental data, whereas reproducibility values above 85% demonstrated satisfactory experimental precision and model robustness.

Table 3. Statistical analysis of regression models.

Parameter	Size	EE
R^2	0.99397	0.97852
R^2 adjusted	0.98311	0.93987
Q^2 (predictive)	0.98314	0.94462
Model validity	0.99802	0.99907
Reproducibility	0.95945	0.85325

III.4. Effect of formulation variables

III.4.1. Effect on niosome size

Cholesterol exhibited a significant positive effect on particle size, with increasing cholesterol concentration leading to the formation of larger vesicles (Figure 2). This behavior can be attributed to the cholesterol-induced rigidification and thickening of the niosomal bilayer, which enhances membrane packing and promotes the formation of more voluminous vesicular structures [12 ,13]. In contrast, sonication time showed a pronounced negative effect on particle size, as prolonged ultrasonic treatment induces vesicle fragmentation, resulting in smaller and more homogeneous particles due to the mechanical disruption of the bilayer structure [15]. Span 60 concentration exerted a moderate negative effect on vesicle size, likely related to its surfactant properties, which favor tighter molecular packing and reduced vesicle dimensions. Furthermore, the interaction between cholesterol concentration and sonication time (X_1X_3) displayed a positive effect, indicating that the membrane-rigidifying influence of cholesterol partially counteracts the size-reducing effect of sonication, thereby limiting vesicle breakdown under ultrasonic energy.

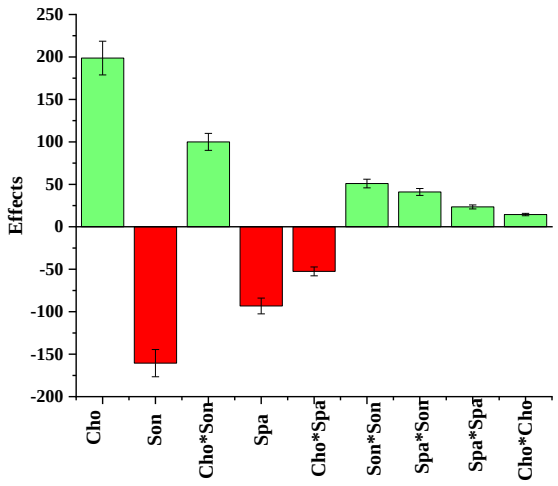

Figure 2. The influence of various factors on the partcile size.

III.4.2. Effect on encapsulation efficiency

Sonication time exhibited the strongest positive effect on encapsulation efficiency (EE), as illustrated in Figure 3. Prolonged sonication enhances homogenization and promotes a more uniform dispersion of the essential oil within the niosomal bilayer, thereby facilitating its effective entrapment within the vesicular structure [16]. The application of ultrasonic energy also contributes to transient bilayer disruption, which may increase membrane fluidity during

formulation, allowing greater incorporation of the essential oil before vesicle stabilization.

Cholesterol concentration also exerted a positive influence on EE by reinforcing the structural integrity of the niosomal bilayer. The presence of cholesterol enhances membrane cohesion and reduces bilayer permeability, thereby limiting the diffusion and leakage of encapsulated compounds and improving overall retention efficiency [17]. However, the quadratic effect of cholesterol (X_1^2) revealed a negative impact on EE at higher concentrations. Excessive cholesterol content can lead to excessive membrane rigidity and reduced free volume within the bilayer, thereby restricting the available space for essential oil incorporation and ultimately lowering encapsulation efficiency.

In contrast, Span 60 demonstrated a significant negative effect on EE. Higher surfactant concentrations are associated with increased bilayer rigidity and tighter molecular packing, which may hinder the accommodation of hydrophobic essential oil molecules within the membrane, thus reducing encapsulation capacity [18]. These findings highlight the importance of optimizing formulation variables to achieve a balanced bilayer structure that maximizes encapsulation efficiency while maintaining vesicle stability.

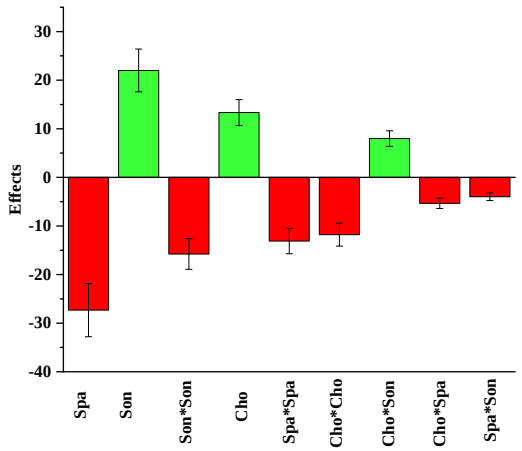

Figure 3. The influence of various factors on the encapsulation efficiency.

III.5. Optimization and validation

The desirability function approach was applied to identify optimal conditions targeting minimum size and maximum EE. The predicted optimal parameters were, cholesterol 2.40 mg/mL, Span 60 5.84 mg/mL, and sonication time 7 min. The predicted responses were 751.6 nm and 92.98% EE. regarding the experimental validation yielded 880 nm and 90.67% EE (Table 4). representing a < 17% deviation for size and < 2.5% for EE,confirming the model's predictive reliability. The slight size discrepancy may be attributed to experimental parameters not included in the model, such as injection rate and organic/aqueous phase ratio [19].

Table 4. Predicted and experimental values for optimized formulation.

Response	Predicted	Experimental	Deviation (%)
Size (nm)	751.58	880	17.1
EE (%)	92.98	90.67	2.5

III.6. FTIR analysis

The FTIR spectra of individual components, physical mixture, placebo, and essential oil-loaded niosomes are presented in Figure 4. The characteristic vibrational bands of each component are clearly identifiable, confirming their structural integrity and enabling the evaluation of potential interactions within the formulation.

Cholesterol exhibited characteristic absorption bands at 3410 cm^{-1} (O-H stretching), 2934 and 2860 cm^{-1} (asymmetric and symmetric CH_2 stretching). 1458 cm^{-1} (CH_2 deformation), 1373 cm^{-1} (symmetric CH_2 bending) and 1055 cm^{-1} (C-C stretching). which are consistent with its steroidal structure enriched in hydroxyl and methylene groups [20]. Span 60 showed typical bands at approximately 3384 cm^{-1} (O-H stretching), 2920-2922 cm^{-1} (aliphatic C-H stretching), 1735 cm^{-1} (ester carbonyl C=O group, confirming its sorbitan monostearate structure), and 1468 cm^{-1} (CH_3 deformation) [21].

The essential oil of Artemisia herba-alba displayed absorption bands at 2920 cm^{-1} (C-H stretching),1625-1596 cm^{-1} and 1614 cm^{-1} (C=C stretching), as well as 1348 cm^{-1}, which are characteristic of terpenic compounds and associated with C=C stretching. carbonyl-related vibrations, and C-H deformation modes [22]. The placebo spectrum represented a simple combination of Span 60 and cholesterol characteristic bands without the appearance of new peaks or significant spectral shifts. confirming the absence of chemical interactions or reactions between excipients. In contrast, for essential oil-loaded niosomes, a noticeable broadening and slight shift of the O-H stretching band around 3400 cm^{-1} was observed, together with modifications in the C-O stretching region between 1675 and 1735 cm^{-1}. These spectral changes suggest the occurrence of hydrogen-bonding interactions between essential oil constituents and the niosomal bilayer. However, the absence of new characteristic absorption bands indicates that the essential oil was physically encapsulated within the vesicular structure without

covalent modification of its chemical structure. These findings are consistent with previous reports on essential oil-loaded niosomal systems [23].

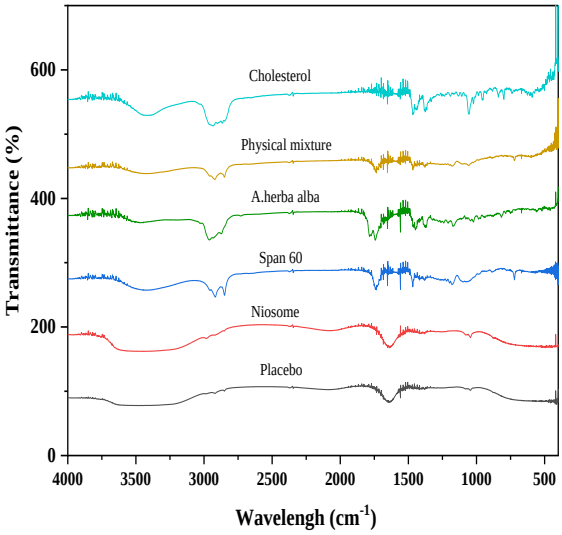

Figure 4. Comparative FTIR analysis of niosomal components, physical mixture,placebo , and essential oil-loaded niosomes.

III.7. XRD characterization

X-ray diffraction (XRD) analysis (Figure 5) revealed distinct crystallographic patterns for each formulation component. Span 60 exhibited a sharp and intense diffraction peak at 2θ = 21-22°. characteristic of its highly ordered crystalline structure associated with tightly packed hydrocarbon chains. Cholesterol also displayed several well-defined diffraction peaks, confirming its crystalline solid-state organization. In contrast, the essential oil showed a broad diffuse halo without distinct peaks consistent with its amorphous liquid nature and absence of long-range molecular order. The physical mixture presented a simple superposition of the individual component patterns without significant peak shifts, indicating the absence of strong molecular interactions prior to formulation. The placebo formulation retained the characteristic Span 60 peak at 21°, although with reduced intensity, suggesting a partial decrease in crystallinity due to bilayer organization. Notably the loaded niosomes exhibited a pronounced reduction in the intensity of the characteristic peaks of both Span 60 and cholesterol. along with peak broadening, indicating a significant loss of crystallinity and increased molecular disorder. This structural changes reflects successful incorporation of the essential oil into the niosomal bilayer. which disrupts the ordered packing of surfactant and cholesterol molecules. The absence of new diffraction peaks further confirms the lack of new crystalline phase formation. demonstrating the physical compatibility of all components within the niosomal system [24-26].

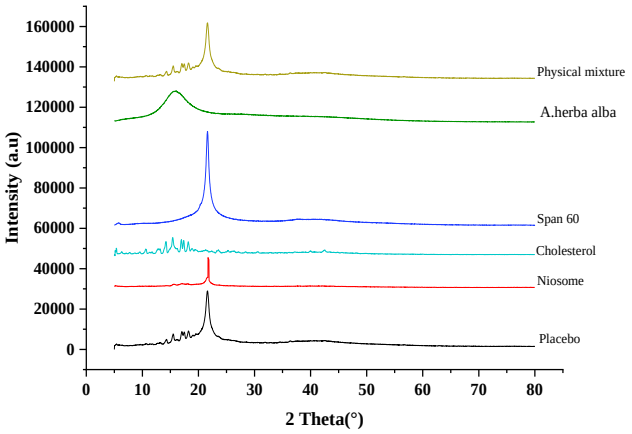

Figure5. XRD diffractograms of pure components (span 60, choelsterol, essential oil) and niosome-loaded essential oil formulation.

III.8. Stability studies

Stability monitoring over 90 days (Table 5. Figure 6) revealed a slight physical instability. A substantial increase in particle size was observed during storage for both placebo and essential oil-loaded niosomal formulations. However, the increase was more pronounced in the loaded vesicles, whose mean diameter rose from approximately 536 nm to 880.27 nm, whereas placebo niosomes exhibited a comparatively lower increase of around 200 nm. This marked difference suggests that the incorporation of essential oil significantly influences the structural organization and physicochemical properties of the niosomal bilayer. Specifically, the presence of lipophilic constituents within the membrane may disrupt the packing arrangement of surfactant molecules, leading to alterations in bilayer fluidity, permeability, and vesicle–vesicle interactions. Such changes can enhance the propensity of vesicles to undergo aggregation and fusion processes during storage, thereby contributing to the observed enlargement in particle size [27]. Importantly, encapsulation efficiency decreased only modestly from 90.67% to 83.40%), indicating that despite physical instability (size growth). the niosomal structure retained most of the encapsulated essential oil. This retention capacity (>80% after 90 days) demonstrates the stabilizing effect of cholesterol and the potential for practical applications [27]. Storage at 4 °C is recommended for future formulations to minimize aggregation [18].

Furthermore, several authors have shown that the stability of niosomes depends heavily on membrane fluidity. An increase in size during storage is generally associated with a decrease in the repulsive forces between particles, as well as with increased mobility of the membrane components, thereby promoting coalescence [18].

This can be attributed mainly to the aggregation and partial fusionof vesicles. Indeed, during storage, inter-vesicular interactions promote theclumping of niosomes, leading to the formation of larger structures.Several studies have reported that an increase in vesicle diameter is a classic indicator of physical instability linked to aggregation and membrane fusion [15,18].

Table 5. Stability data of optimized niosomal formulation.

Time (days)	Placebo size (nm)	Loaded size (nm)	EE (%)
0	536	880	90.67
15	870	1200	90.30
30	1340	1770	88.77
60	1750	2350	86.50
90	2200	2780	83.40

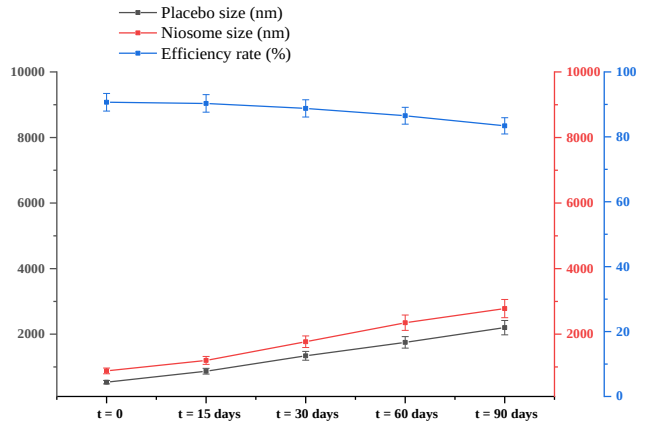

Figure 6. Stability evaluation of niosomal formulations via particle size and encapsulation efficiency during storage.

IV. Conclusions

This study successfully developed and optimized niosomal formulations for Artemisia herba-alba essential oil using a Box-Behnken experimental design. The optimized formulation (cholesterol 2.40 mg/mL, Span 60 5.84 mg/mL, sonication time 7 min) achieved 90.67% encapsulation efficiency with 880 nm particle size. Characterization through FTIR confirmed physical encapsulation via hydrogen bonding without chemical modification, while XRD demonstrated reduced crystallinity indicating essential oil integration into the bilayer. Stability studies revealed acceptable retention (> 83% EE) despite physical aggregation over 90 days.

These results establish niosomes as an effective delivery system for A. herba-alba essential oil, addressing limitations of volatility and instability while preserving therapeutic potential. The quality-by-design approach enabled systematic optimization and predictive modeling, providing a robust framework for future scale-up.

Future investigations should focus on extending the physicochemical and biocompatibility assessment of the developed niosomal system, including detailed release behavior and stability under controlled storage conditions. In addition, the use of complementary analytical techniques such as dynamic light scattering (DLS) would allow more accurate determination of hydrodynamic particle size, polydispersity index (PDI), and zeta potential, thereby strengthening the physicochemical characterization of the formulation. Further biological evaluations will be necessary to fully establish the potential applicability of this system in pharmaceutical or nutraceutical contexts.

Acknowledgments
The authors thank the Direction Générale de la Recherche Scientifique et Développement Technologique of Algeria for support.

Conflict of interest
The authors declare no conflict of interest.

Funding
This research received no external funding.

References:

1. S. Burt. Essential oils: their antibacterial properties and potential applications in foods: A review. International Journal of Food Microbiology 94(3), 223–253, 2004. https://doi.org/10.1016/j.ijfoodmicro.2004.03.022

2. M. Saida, R. Essid, S. Jellouli, N. Fares, A. Delimi, A. Amrani, O. Tabben. Algerian Artemisia herba-alba (Asso): extract and essential oils investigation. Natural Product Communications 19(9), 1934578X241282821, 2024. https://doi.org/10.1177/1934578X241282821

3. F. Lazreg, Z. Benaouf, A. Merzoug, et al. Essential oil study of Artemisia herba-alba (Asso.): Antifungal activity against Fusarium oxysporum f. sp. ciceri and phytochemical analysis by GC-MS. Plants 14(5), 892, 2025. https://doi.org/10.3390/plants14050892

4. F. Bakkali, S. Averbeck, D. Averbeck, M. Idaomar. Biological effects of essential oils: A review. Food and Chemical Toxicology 46(2), 446–475, 2008. https://doi.org/10.1016/j.fct.2007.09.106

5. R. Khan, R. Irchhaiya. Niosomes: A potential tool for novel drug delivery. Journal of Pharmaceutical Investigation 46(3), 195–204, 2016. https://doi.org/10.1007/s40005-016-0234-9

6. S. Moghassemi, A. Hadjizadeh. Nano-niosomes as nanoscale drug delivery systems: An illustrated review. Journal of Controlled Release 185, 22–36, 2014. https://doi.org/10.1016/j.jconrel.2014.04.015

7. R. Sharma, J. S. Dua, D. N. Parsad. An overview on niosomes: Novel pharmaceutical drug delivery system. Journal of Drug Delivery and Therapeutics 12, 171–177, 2022. https://api.semanticscholar.org/CorpusID:248447719

8. A. A. Bautista Solano, A. Martínez-Arce, D. Díaz, et al. Optimization and synthesis of nano-niosomes for encapsulation of triacontanol by Box–Behnken design. Molecules 29(18), 4421, 2024. https://doi.org/10.3390/molecules29184421

9. S. Soni, K. Khatri, C. P. Jain. Size-dependent effects of niosomes on the penetration of methotrexate in skin layers. Future Journal of Pharmaceutical Sciences 10(1), 47, 2024. https://doi.org/10.1186/s43094-024-00624-2

10. N. Ullah, S. Ullah, J. Ali, et al. Fabrication and optimization of essential-oil-loaded nanoemulsion using Box–Behnken design against Staphylococcus aureus and Staphylococcus epidermidis isolated from the oral cavity. Pharmaceutics 14(8), 1640, 2022. https://doi.org/10.3390/pharmaceutics14081640

11. K. El Ouahdani, I. Es-Safi, H. Mechchate, et al. Thymus algeriensis and Artemisia herba-alba essential oils: Chemical analysis, antioxidant potential, in vivo anti-inflammatory and analgesic activities, and acute toxicity. Molecules 26(22), 6780, 2021. https://doi.org/10.3390/molecules26226780

12. O. R. Estupiñan, P. Garcia-Manrique, M. D. C. Blanco-Lopez, M. Matos, G. Gutiérrez. Vitamin D_3 -loaded niosomes and transfersomes produced by ethanol injection method: Identification of the critical preparation step for size control. Foods 9(10), 1367, 2020. https://doi.org/10.3390/foods9101367

13. S. Fatmi, Z. Toutou, N. Chibani, H. A. Lezrag, M. Skiba, M. Iguerouada. Optimization and formulation of mixed niosome/cyclodextrin encapsulation process for Béjaia propolis extract. Biopolymer Applications Journal 3(2), 12–17, 2024. https://univ-bejaia.dz/revue/baj/article/view/538

14. S. Fatmi, L. Taouzinet, A. Benslimane, N. Chibani, D. Hammiche. Drug release and sperm motility protection studies of vitamin E encapsulated in liposome, cyclodextrin, or polyethylene glycol. Materials Today: Proceedings 53, 71–75, 2022. https://doi.org/10.1016/j.matpr.2022.01.014

15. F. Nowroozi, A. Almasi, J. Javidi, A. Haeri, S. Dadashzadeh. Effect of surfactant type, cholesterol content, and various downsizing methods on the particle size of niosomes. Iranian Journal of Pharmaceutical Research 17(Suppl.), 70–82, 2018.

16. S. Shiri, K. Gharanjig, M. Hosseinnezhad, A. Tahghighi, M. Etezad. Exploring the use of saponin as a biosurfactant for formulating niosomal carriers to regulate the release of berberine. Journal of Dispersion Science and Technology, 1–11, 2025. https://doi.org/10.1080/01932691.2025.2462691

17. A. A. Revankar, A. S. Patil, R. Karishetti, et al. Enhanced bioavailability of quercetin-loaded niosomal in situ gel for the management of Parkinson's disease. Frontiers in Pharmacology 15, 1519649, 2025. https://doi.org/10.3389/fphar.2024.1519649

18. V. B. Junyaprasert, V. Teeranachaideekul, T. Supaperm. Effect of charged and nonionic membrane additives on physicochemical properties and stability of niosomes. AAPS PharmSciTech 9(3), 851–859, 2008. https://doi.org/10.1208/s12249-008-9123-3

19. O. R. Estupiñan, P. Garcia-Manrique, M. D. C. Blanco-Lopez, et al. Vitamin D_3 -loaded niosomes and transfersomes produced by ethanol injection. Colloids and Surfaces B: Biointerfaces 196, 111363, 2020. https://doi.org/10.1016/j.colsurfb.2020.111363

20. B. J. Ha, S. Park. Classification of gallstones using Fourier-transform infrared spectroscopy and photography. Biomaterials Research 22, 24, 2018. https://doi.org/10.1186/s40824-018-0140-4

21. A. B. Darwish, A. Salama, I. Essam Ibrahim Al-Samadi. Formulation, optimisation, and evaluation of lornoxicam-loaded novasomes for targeted ulcerative colitis therapy: In vitro and in vivo investigations. Journal of Drug Delivery Science and Technology 91, 106184, 2025. https://doi.org/10.1016/j.jddst.2025.106184

22. A. Ez-Zoubi, Y. Ez Zoubi, F. Bentata, et al. Preparation and characterization of a biopesticide based on Artemisia herba-alba essential oil encapsulated with succinic acid-modified β-cyclodextrin. Journal of Chemistry 2023(1), 3830819, 2023. https://doi.org/10.1155/2023/3830819

23. M. Ebrahimpour, M. Akhlaghi, M. Hemati, et al. In vitro evaluation and comparison of anticancer, antimicrobial, and antifungal properties of thyme niosomes containing essential oil. Nanomedicine Journal 9(4), 258–268, 2022. https://doi.org/10.22038/NMJ.2022.66932.1707

24. H. A. Lezrag, S. Fatmi, L. Taouzinet, et al. Improving camphor solubility and stability through α-cyclodextrin encapsulation: Characterization, cytotoxicity investigation, and bull sperm preservation evaluation. Journal of Inclusion Phenomena and Macrocyclic Chemistry 105(9), 537–548, 2025. https://doi.org/10.1007/s10847-025-01308-x

25. Z. Sezgin-Bayindir, N. Yuksel. Investigation of formulation variables and excipient interaction on the production of niosomes by factorial design. Journal of Liposome Research 22(3), 207–218, 2012. https://doi.org/10.3109/08982104.2011.641547

26. P. Kadiroglu, B. Kılınçlı, C. Ilgaz, et al. Nanoencapsulation of hydroxytyrosol extract of fermented olive leaf brine using proniosomes. Journal of the Science of Food and Agriculture 105(15), 8477–8488, 2025. https://doi.org/10.1002/jsfa.70087

27. J. M. V. de Vilela, F. A. Oliveira, M. B. C. de Oliveira, et al. Safety of lavender oil-loaded niosomes for in vitro culture and biomedical applications. Pharmaceutics 14(7), 1454, 2022. https://doi.org/10.3390/pharmaceutics14071454

28. H. Vardhan, M. Bajpai, S. Verma, et al. Niosomes in drug delivery. Asian Journal of Research in Pharmaceutical Sciences 15(1), 7–15, 2025. https://doi.org/10.52711/2231-5659.2025.00002